Gain Measurement of 10.6 μm CO_2 Gasdynamic Laser Driven by High Temperature Reaction of CO-N_2O-H_2 in Shock Tube*

Nobuyuki FUJII**, Toshihiko TOKUDA**, Naoki SAKATSUME**,
Yoshio NOSAKA** and Hajime MIYAMA**

Basic study of CO_2 gasdynamic laser (GDL) was carried out by a conventional pressure driven shock tube equipped with a supersonic nozzle section. Population inversion of the vibrational levels of CO_2 in an expanding flow of mixture produced by high temperature reaction of CO-N_2O-H_2 system behind a shock wave was observed by measuring 10.6 μm small-signal-gain. The experimental data were compared with those obtained by computer simulation assuming quasi-one-dimensional steady flow in the nozzle and three vibrational mode model. As a reservoir condition in the simulation, kinetics of CO_2 formation in CO-N_2O-H_2 system behind the reflected shock wave was discussed.

Key words: shock tube/CO_2 gasdynamic laser/population inversion/CO-N_2O-H_2 reaction

1. Introduction

The practical operating CO_2 gasdynamic laser (GDL) is that driven by the combustion of fuels in which the required components for the laser media were produced at temperature and pressure compatible with reasonably efficient operation. In the past several decades extensive studies of CO_2 GDL using chemical combustion have been carried out[1]. Unfortunately neither the mixture ratio of combustion products nor the reservoir temperature and pressure are independent of each other for such combustion driven GDLs.

It has been reported that $CO+N_2O$ reaction creates highly nonequilibrium pumping of vibrational levels of CO_2 and enhances the gain coefficient due to the direct conversion of chemical energy into laser radiation[2)~4)]. However, such higher gain has not been obtained in a similar experiment repeated by the authors[5] who have also found that the addition of a small amount of hydrogen to the mixture increased the gain, which is consistent with the observations by Kudryavtsev et al[6].

It is known that the formation of CO_2 in CO-N_2O mixture at high temperature is due to the following two exothermic reactions; direct exchange reaction $CO+N_2O \rightarrow CO_2+N_2+365.3$ (kJ. mol^{-1}) and recombination reaction $CO+O+M \rightarrow CO_2+M+523$ (kJ. mol^{-1}). Previously, the authors investigated $CO-N_2O$ reaction by measuring infrared emission of CO_2 produced behind reflected shock waves and reported the rate constants for those reactions[7),8)]. Also, it was found that the addition of a small amount of H_2 to $CO-N_2O$ system had a serious effect upon the reaction rate measurement and that CO_2 formation through exothermic exchange reaction $CO+OH \rightarrow CO_2+H+104.6$ (kJ. mol^{-1}) became more important than the two reactions described above[9].

In the present study, using a shock tube with a nozzle section, population inversion between vibrational energy levels of CO_2 in an expanding flow of mixtures produced by the reaction of $CO-N_2O-H_2$ system behind a reflected shock wave was observed by measuring 10.6 μm small-signal-gain for the $CO_2(001)-(100)$ transition. The gains were compared with those of non-reacting CO_2-N_2 system at various initial temperatures (T_{50}). Further, the gains were compared with those of simulations by assuming quasi-one dimensional steady flow in

Received March 24, 1988

* A part of this paper was reported at 25th Combustion Symposium Japan (1987).

** Department of Chemistry, Nagaoka University of Technology

the nozzle and three vibrational mode model of CO_2 -N_2 system.

2. Experimental

The shock tube is made of stainless steel of 78 mm inner diameter consisting of a driver section 1.5 m long and a driven section 3.6 m long and is connected to a nozzle section. A two-dimensional wedge nozzle with 1 mm throat height, 10 deg. half angle, 78 mm width and 162 mm length is connected at the end of the driven section. A 58×78 mm square tube 35 cm long and a dump tank are connected to the nozzle section. A schematic diagram of the experimental apparatus used is shown in Fig. 1.

In the experiment, shock wave was generated by bursting a polyester diaphragm with a plunger and a secondary thin polyester diaphragm mounted between the end of the shock tube and the nozzle was burst by the reflected shock wave to generate an expansion flow through the nozzle. The incident shock wave velocity was measured by four piezoelectric gauges located at intervals of 300 mm and a time counter. Temperature (T_{50}) and pressure (P_{50}) just behind the reflected shock wave were calculated from the incident shock velocity using the conventional method[10].

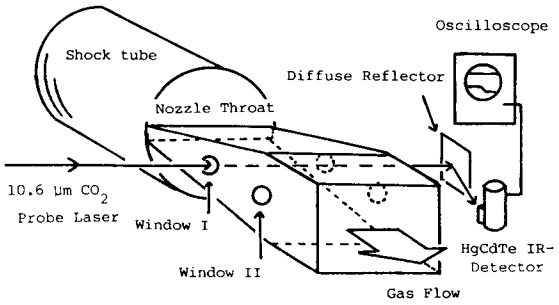

Fig. 2 A schematic of the instrument for gain measurement.

The 10.6 μm small-signal-gain measurement was made at 86 mm (window I) or 162 mm (window II) down stream from the nozzle throat. A beam of low power CO_2 probe laser was directed through the expansion flow and the amplified beam was reflected by a diffuse plate and detected by a HgCdTe detector and the signal was displayed on a digital oscilloscope. A schematic diagram of the instrumentation for gain measurement is shown in Fig. 2.

The experimental conditions are shown in

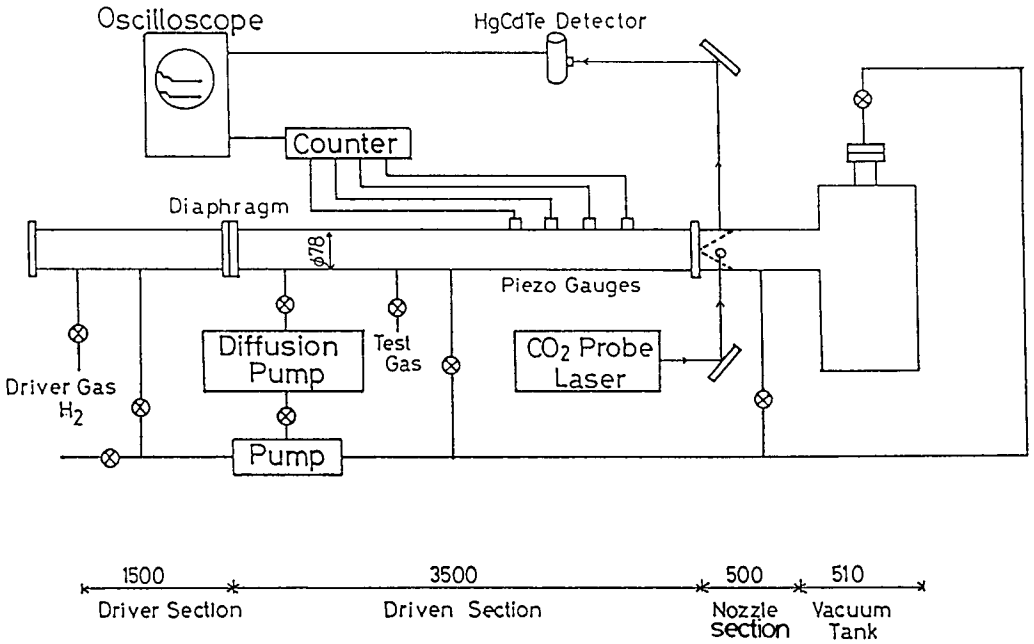

Fig. 1 A schematic of the shock tube for gasdynamic laser experiment.

Table 1. Experimental condition

1. Composition

	CO_2	CO	N_2O	N_2	He	H_2
a.	5			55	40	
b.		5	5	50	40	
c.		5	5	50	39	1

2. Reflected shock temperature range 1200−2400 K, P=4 atm constant

Table 1. The gases used in the experiments were obtained from commercial suppliers and the purities of the gases were as follows; CO: 99.9% (O_2, H_2 < 100 ppm, H_2O < 15 ppm), N_2O: 98% (O_2 < 1.4%, N_2 < 0.6%, H_2O < 600 ppm), N_2: 99.9999%, He: 99.9995%. These gases were used without further purification.

3. Simulation for Small-signal-gain

The transition between the upper level CO_2(001) and the lower level CO_2(100) yields laser radiation at 10.6 μm. The relationship between a population inversion of vibrational levels and a small signal gain is expressed as follows[1],

$$G_0 = (\lambda^2/4\pi\tau_{lu}Z)((g_l/g_u)N_u - N_l)$$

where G_0 is the small-signal-gain, λ is the wave length, τ_{lu} is the radiative life time, Z is the molecular collision frequency, N_l and N_u are the numbers of molecules per unit volume in the lower and the upper levels (shown by suffix l and u, respectively) and also, g_l and g_u are statistical weights of the levels. When a population inversion exists between the levels, the small-signal-gain is positive.

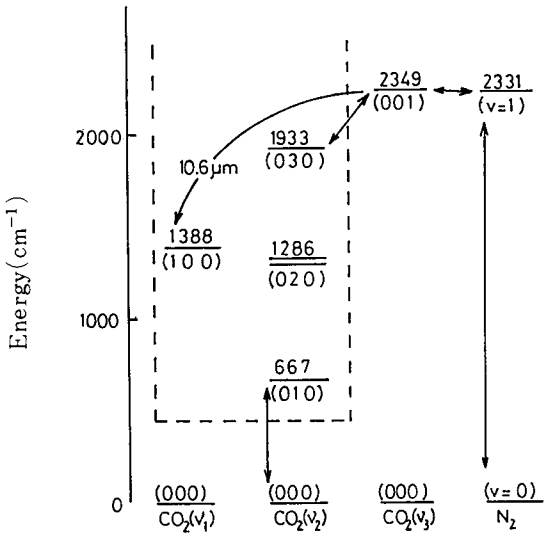

Fig. 3 A vibrational kinetic model for CO_2-N_2 system[1].

Table 2. Energy transfer parameters

	M	a	b	c	d
k_1	CO_2, N_2O	−262.3	200.4	−66.51	−7.971
	N_2	−257.7	141.4	−54.22	−8.701
	H_2	−825.8	404.3	−65.27	−8.347
	H_2O	−732.8	398.7	−65.40	−7.780
	O_2, CO, NO	−301.3	238.2	−79.05	−7.270
	He	−261.8	107.1	−31.37	−9.701
k_2	CO_2, N_2O	−2497.0	1134.0	−186.2	−3.071
	N_2	−2138.0	1025.0	−176.2	−3.903
	H_2			−15.0	−10.72
	H_2O	1129.0	−576.2	94.35	−17.08
	O_2, NO	−51.93	131.7	−55.70	−8.925
	CO	−806.8	489.7	−106.4	−6.567
	He	−1554.0	811.7	−153.5	−4.637
k_3	CO_2, N_2O	−282.0	150.4	−127.7	−6.005
	N_2, O_2, CO, NO	−282.0	150.4	−127.7	−6.005
	H_2			−41.0	−9.400
	H_2O	−286.3	152.0	−62.57	−7.366
	He			−47.6	−9.520
k_4		−1870.0	864.3	−121.6	−7.153

$\log(k_i) = aT^{-1} + bT^{-2/3} + cT^{-1/3} + d$ (in units of $cm^3\ part^{-1}s^{-1}$)
$1/\tau_i = k_i \times P/kT$, τ_i: relaxation time

The gain was calculated numerically as follows. For the gas mixture flow expanded from the nozzle, the fundamental equations for the quasi-one dimensional, chemically frozen and vibrationally nonequilibrium flow were assumed.

As the energy transfer processes, the following equations were used by assuming three vibrational energy mode model[1] as shown in Fig. 3. In the model, it is assumed that a near Boltzmann distribution exits in each mode, and that the ν_1 and ν_2 modes are in local equilibrium to be closely coupled.

$CO_2(010) + M = CO_2(000) + M$: τ_1
$CO_2(001) + M = CO_2(030) + M$: τ_2
$N_2(v=1) + M = N_2(v=0) + M$: τ_3
$CO_2(001) + N_2(v=0) = CO_2(000) + N_2(v=1)$: τ_4

Here, τ_i is the relaxation time for the above energy transfer process i, and is related to the rate constant

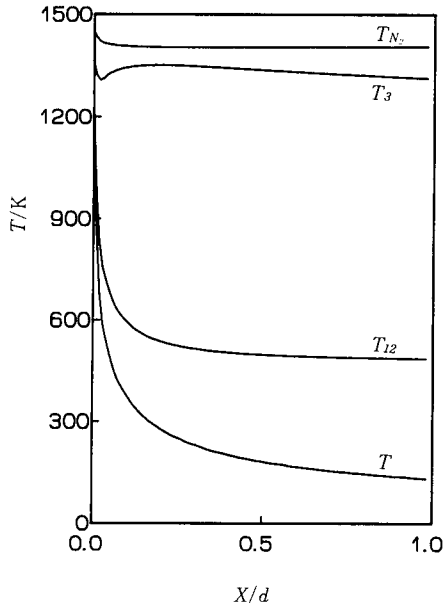

Fig. 4 An example of steady-state vibrational and translational temperature distributions through the nozzle obtained by the numerical simulation. T_{N_2}, T_3 are the vibrational temperatures of N_2 and ν_3, respectively, and T_{12} is the combined vibrational temperature of ν_1 and ν_2. T is the translational temperature. The distance is normalized with the nozzle length d. $T_{50}=1500$ K and $P_{50}=4.0$ atm.

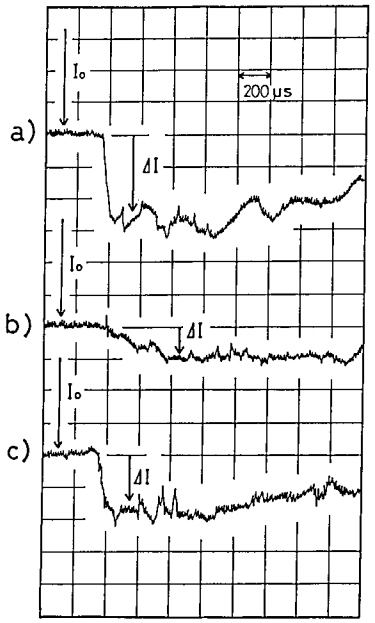

Fig. 5 Comparison of profiles of 10.6 μm small signal gain.
a) CO_2-N_2 (mixture a), $T_{50}=1774$ K, $P_{50}=3.9$ atm,
b) CO-N_2O (mixture b), $T_{50}=1748$ K, $P_{50}=4.1$ atm,
c) CO-N_2O-H_2 (mixture c), $T_{50}=1748$ K, $P_{50}=4.1$ atm,
I_0 is about 12 divisions.

k_i via a relation; $1/\tau_i = k_i P/kT$, where k is the Boltzmann constant. The value of k_i is an average value of the rate constants for collision partners M of i group shown in Table 2. In the table, the coefficients for the temperature polynominal[11] of the rate constants are shown for the collision partners[12], where the coefficient for N_2O is assumed to be the same as that for CO_2 and those for CO and NO are assumed to be equal to that for O_2. As the reservoir condition, the "quasi-equilibrium" condition obtained by numerical calculation for reaction system behind the reflected shock wave was used. The Runge-Kutta-Gill method was used to solve these equations[11]. Steady state vibrational temperature and number density distributions were calculated and small-signal-gain was obtained by using above equations. An example of the temperature distribution is shown in Fig. 4.

4. Results and Discussion

In the experiment, the population inversion of CO_2 vibrational levels in the nozzle flow was studied by measurement of small-signal-gain using 10.6 μm CO_2 probe laser. The gain was obtained from the equation $(I_0+\Delta I)/I_0 = \exp(G_0 L)$, where I_0 is incident radiation intensity of CO_2 probe paser, ΔI is the change in the beam intensity after traversing the nozzle flow, and L is the optical path length through the flow.

Typical profiles of the amplified probe laser radiation intensity through nozzle flow for the mixtures heated behind the reflected shock waves are shown in Fig. 5. The intensity I_0 of the probe laser increased abruptly by ΔI for CO_2-N_2 mixture as shown in Fig. 5(a), but the intensity increased very slowly for $CO-N_2O$ mixture as shown in Fig. 5(b). However, the addition of H_2 to $CO-N_2O$ mixture makes the rise time of gain profile very fast

as shown in Fig. 5(c). This is partly due to the acceleration of CO_2 formation by H_2-O_2 reaction as reported elsewhere[9].

Stationary values of the small-signal-gain G_0 for the three mixtures were plotted against the reflected shock temperature (T_{50}). The temperature dependences of G_0 obtained at window I and II of the nozzle (86 and 162 mm from the nozzle throat, respectively) for $CO-N_2O$ mixture and $CO-N_2O-H_2$ mixture are compared with that for CO_2-N_2 mixture as shown in Figs. 6 and 7. The comparison shows that values of G_0 of mixture (c) at window I are larger than those of mixture (b), (at constant pressure P_{50} = 4.0±0.2 atm). This was due to the difference of CO_2 formation rate with and without H_2 in $CO-N_2O$ mixture as described previously.

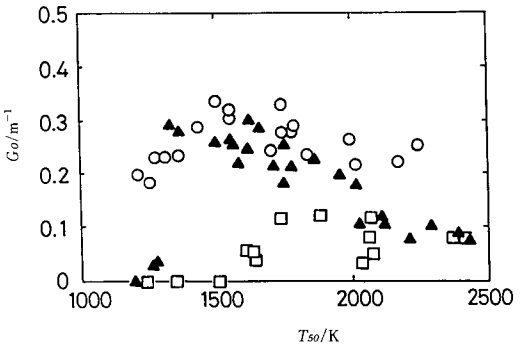

Fig. 6 Temperature (T_{50}) dependence of small-signal-gain measured at window I, P_{50}=4.0±0.2 atm. (○ : mixture a, □ : mixture b, ▲ : mixture C)

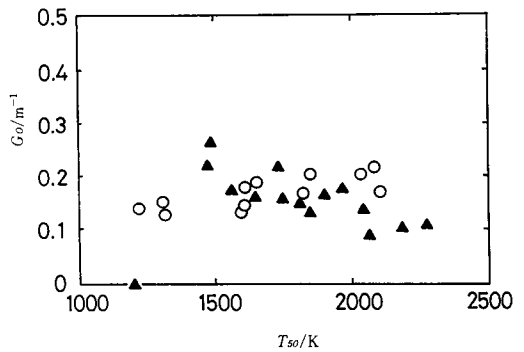

Fig. 7 Temperature (T_{50}) dependence of small-signal-gain measured at window II, P_{50}=4.0±0.2 atm. (○ : mixture a, ▲ : mixture C)

The G_0 values of mixture (c) at window I do not exceed the values of mixture (a). However, the value of G_0 of mixture (c) at window II seems to be larger than that of mixture (a) at about T_{50} = 1500 K.

Simulation of small-signal-gain was carried out for CO_2-N_2 mixture at first. Temperature and pressure dependences of the calculated gain agreed well with the experimental values[9] and they were almost the same as those reported by other researchers[1]. In order to simulate the gain for the reaction system $CO+N_2O+H_2$ numerically, it is necessary to know the reaction processes behind the shock wave. The mechanism of the high-temperature reaction of $CO-N_2O-H_2$ system was studied in the previous work and the rates of the main reactions were already checked[7]~[9]. Calculation of reaction behind the shock wave was performed by using the reaction mechanism in Table 3. In this calculation, differential equations for reactions (1)−(12) and their reverse reactions were solved numerically, coupled with a heat balance equation and gas flow equations for the reflected shock wave. An example of the calculated concentration profiles of main species and the calculated temperature and pressure changes are shown in Fig. 8. It is shown that quasi-equilibrium is attained at about 300 μsec after the arrival of shock wave in this case. Also, the calculated changes of temperature and pressure were about 500 K and 1.5 atm at 300 μsec, respectively. Calculated values of mole percent of main

Table 3. Reaction Scheme and Rate Paramcters*)

No.	Reaction	log A	B	E/kJ	Ref.
(1)	$N_2O+CO = N_2+CO_2$	10.99	0	73.0	[8]
(2)	$N_2O+M = N_2+O+M$	15.21	0	257.7	[15]
(3)	$N_2O+O = N_2+O_2$	14.00	0	117.2	[14]
(4)	$N_2O+O = NO+NO$	13.84	0	111.3	[14]
(5)	$NO_2+O = NO+O_2$	13.30	0	4.6	[16]
(6)	$CO+O+M = CO_2+M$	15.20	0	30.0	[8]
(7)	$NO+O+M = NO_2+M$	14.95	0	−7.5	[16]
(8)	$H_2+O = OH+H$	7.18	2.0	31.6	[13]
(9)	$H_2+OH = H_2O+H$	8.00	1.6	13.8	[13]
(10)	$O_2+H = OH+O$	17.08	−0.9	69.1	[13]
(11)	$N_2O+H = N_2+OH$	14.20	0	62.8	[17]
(12)	$CO+OH = CO_2+H$	6.64	1.5	−3.1	[13]

*) $k=AT^B\exp(-E/RT)$ (in units of $cm^3\ mol^{-1}$ and s^{-1})

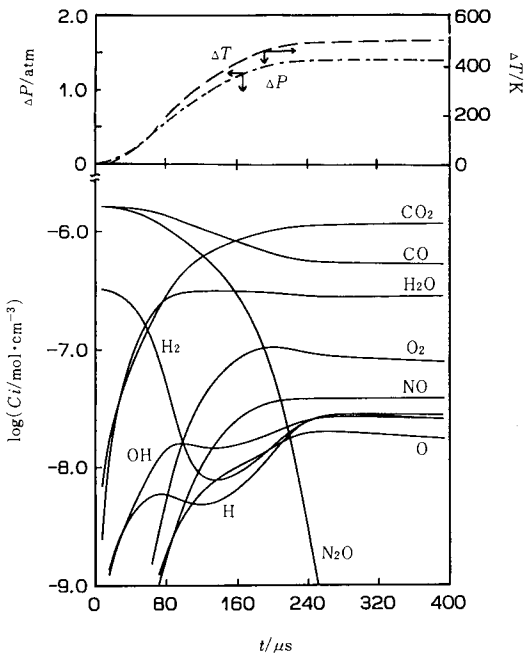

Fig. 8 An example of calculated concentration profiles and temperature and pressure profiles for $CO-N_2O-H_2$ system. $T_{50}=1500$ K, $P_{50}=4.0$ atm.

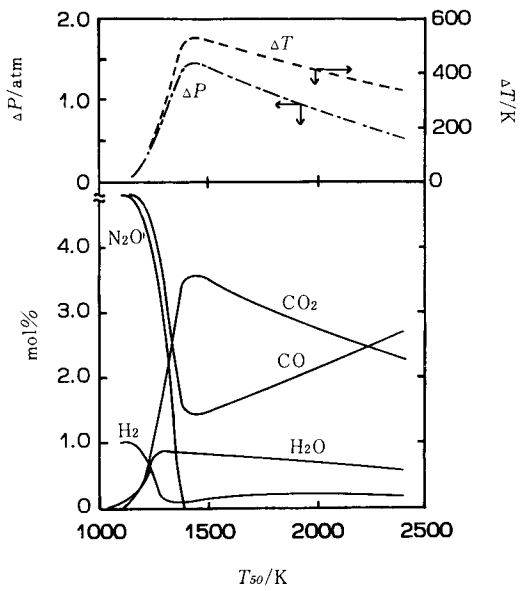

Fig. 9 Calculated concentrations of species and temperature and pressure at $t=300\,\mu$s for $CO-N_2O-H_2$ system. $T_{50}=1500$ K, $P_{50}=4.0$ atm.

species in the mixture and also temperature and pressure changes at 300 μ sec on various temperature for mixture (c) are shown in Fig. 9. It is found that the reaction does not proceed enough within 300 μ sec below about 1300 K under the present experimental conditions. Accordingly, the low G_0 values of mixture (c) below 1300K shown in Figs. 6 and 7 were explained by the calculation of reaction.

Simulations of G_0 for mixture (c) were performed by using the values at 300 μsec as reservoir condition and the typical results are shown in Fig. 9. Temperature dependence of G_0 obtained by the simulation were compared with experimental values. The numerically simulated values agreed well with the experimental values at the window I and II, as shown in Figs. 10 and 11, respectively.

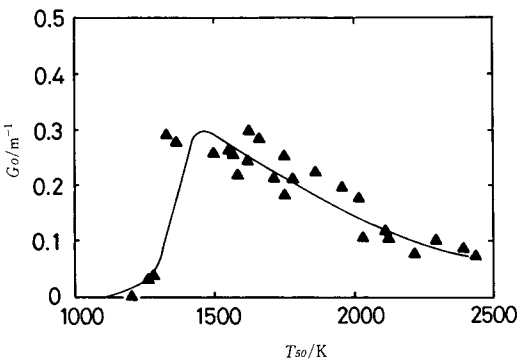

Fig. 10 A comparison between the experimental and calculated dependence of the small-signal-gain on T_{50} for $CO-N_2O-H_2$ system at window I.

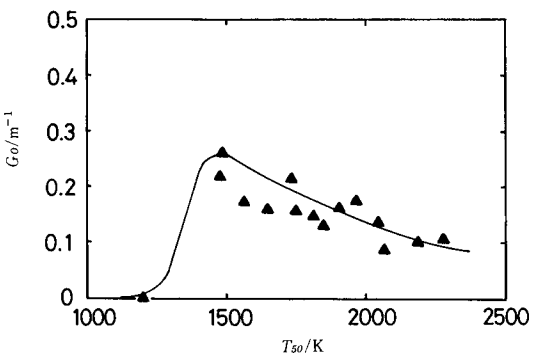

Fig. 11 A comparison between the experimental and calculated dependence of the small-signal-gain on T_{50} for $CO-N_2O-H_2$ system at window II.

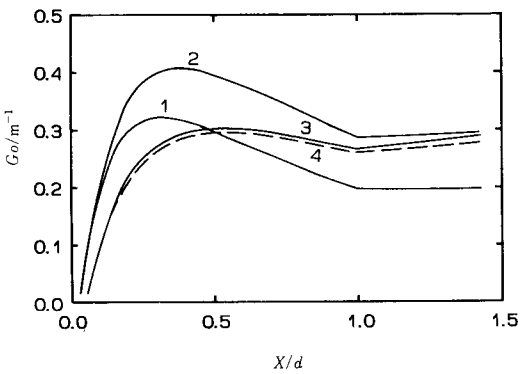

Fig. 12 Comparison of the calculated distribution of gains along nozzle axis.

line	mixture	CO_2(%)	H_2O(%)	T(K)
(1)	CO_2-N_2	5	0	1500
(2)	CO_2-N_2-H_2O	5	1	1500
(3)	CO_2-N_2-H_2O	5	1	2000
(4)	CO-N_2O-H_2	~3.5	~1	2000

In order to evaluate the characteristics of the CO_2 gasdynamic laser using the reaction of $CO-N_2O-H_2$ mixture, i) effect of H_2O addition to CO_2-N_2 mixture and ii) effect of the temperature rise due to the reaction on gains were calculated. The calculated values of small-signal-gain distribution by various models were compared as shown in Fig. 12, where reservoir condition of each model is described in the figure caption. The distribution of gain for $CO-N_2O-H_2$ mixture is shown by line 4 in the figure. From the comparison of the value for CO_2-N_2 (line 1) with that for $CO_2-N_2-H_2O$ (line 2), it is obvious that H_2O addition to CO_2-N_2 system causes a marked increase of small-signal-gain. This seems to be mainly due to the increase of relaxation of the lower vibrational levels of CO_2 by H_2O[1]. From the comparison of the value of line 1 with that for $CO_2-N_2-H_2O$ mixture (line 3), it is found that temperature rise has small negative effect on small-signal-gain, but it was found that the value of line 3 is larger than the value of line 1 at nozzle end (X/d = 1.0). This tendency agreed with the experimental one as shown in Fig. 11.

5. Conclusion

Higher small-signal-gain was not obtained for CO-N_2O system compared with that for CO_2-N_2 system. However, addition of H_2 to the former system increased appreciably the small-signal-gain. This phenomenon can be explained by the chemical kinetics of $CO-N_2O-H_2$ system and also by the effect of H_2O produced on the relaxation of the CO_2 lower vibrational levels. However, it is not found that chemical non-equilibrium pumping suggested by Kudryavtsev et al[3),4)] occurred by the reaction in shock tube.

Acknowledgment

The authors wish to express their thanks to Dr. W. Masuda of their university for his helps on the computer simulations, and to Mr. K. Mitomi of their university for his assistance on the construction of the experimental apparatus.

References

1) Anderson, J.D. Jr.: Gasdynamic Lasers ; An Introduction, Academic Press, 1976.
2) Kudryavtsev, N.N., Novikov, S.S. and Svetlichnyi, I.B.: *Sov. Phys. Dokl.* **19**, 831 (1975).
3) Kudryavtsev, N.N., Novikov, S.S. and Svetlichnyi, I.B.: *Sov. Phys. Dokl.* **21**, 748 (1976).
4) Kovtun, V.V., Kudryavtsev, N.N., Novikov, S.S., Svetlichnyi, I.B. and Shagov, P.N.: *Sov. Phys. Dokl.* **23**, 503 (1978).
5) Miyama, H., Takeishi, T., Kakuda, T., Nosaka, Y. and Fujii, N.: *Symposium on Gas-Flow Lasers and Chemical Lasers*, p. 24, Institute of Laser & Chemical Technology, 1986.
6) Kudryavtsev, N.N. and Soloukhin, R.I.: *Fifth Gas Flow and Chemical Lasers Symposium*, p. 425, Adam Hilger Ltd., 1984.
7) Fujii, N., Kakuda, T., Sugiyama, T. and Miyama, H.: *Chem. Phys. Lett.* **122**, 489 (1985).
8) Fujii, N., Kakuda, T., Takeishi, N. and Miyama, H., *J. Phys. Chem.* **91**, 2144 (1987).
9) Miyama, H., Fujii, N., Takeishi, N., Tokuda, T. and Sakatsume, N.: *Laser and Particle Beams*, (in press).
10) Gardiner, W.C. Jr.: Shock Wave in Chemistry (Lifshitz, A. Ed.), p. 319, Marcel Dekker, 1981.

11) Yamada, H. and Masuda, W.: *Trans. Japan Soc. Aero. Space Sci.* **26**, 74 (1985).
12) Taylor, R.L. and Bitterman, S.: *Rev. Mod. Phys.* **41**, 26 (1969).
13) Warnatz, J.: Combustion Chemistry (Gardiner, W. C. Jr. Ed.), p. 197 Springer Verlag, 1984.
14) Hanson, R.K. and Salimian, S.: Combustion Chemistry (Gardiner, W.C. Jr. Ed.), p. 361, Springer Verlag, 1984.
15) Fujii, N., Sato, H., Fujimoto, S. and Miyama, H.: *Bull. Chem. Soc. Jpn.*, **57**, p. 277 (1984).
16) Milks, D. and Matula, R.A.: *Fourteenth Symposium (International) on Combustion*, p. 83 (1973).
17) Hidaka, Y., Takuma, H. and Suga, M.: *Bull. Chem. Soc. Jpn.*, **58**, p. 291 (1985).